

Electronic Supporting Information for:

One-pot synthesis of two-dimensional multilayered graphitic carbon nanosheets by low-temperature hydrothermal carbonization and aids of *in-situ* formed copper as template and catalyst

S1: Synthesis of two-dimensional graphitic carbon nanosheets

Two-dimensional graphitic carbon nanosheets were synthesized by hydrothermal method as follows: 0.30 g $\text{CuSO}_4 \cdot 5\text{H}_2\text{O}$ was firstly dissolved in 40 mL H_2O , and then 0.05g dried leaves were added into it as a whole part. Then the above mixture was transferred into a 50 mL Teflon-lined stainless-steel autoclave and heated in oven at 150-300 °C for 24 hours. After hydrothermal process, the as-prepared products were collected and washed several times with deionized water and ethanol by centrifugation at 5000 rpm for 3 min, and then dried under vacuum at 65 °C. The obtained products synthesized under 150, 200, 250, and 300 °C were named Product-1, Product-2, Product-3, and Product-4, respectively. Furthermore, in order to obtain two-dimensional carbon nanosheets, the as-prepared products were firstly reacted with diluted nitric acid fully, and then washed by vacuum filtration with deionized water several times to obtain solid product, and finally dried under vacuum at 65 °C. Corresponding to the product synthesized under temperature of 150, 200, 250, and 300 °C, the obtained carbon nanosheets were named CS-1, CS-2, CS-3, and CS-4. For comparison, the experiment without adding $\text{CuSO}_4 \cdot 5\text{H}_2\text{O}$ were also conducted under the temperature of 150, 200, 250, and 300 °C. Instead of *Pachira aquatica* Aubl leaves, biomass of *Pachira aquatica* Aubl petioles (leaf stalks) and bamboo leaves were also taken as carbon precursor with the same experimental conditions for hydrothermal reaction under 300 °C. Correspondingly, the obtained products were named Product-5 and Product-6, and the obtained carbon nanosheets were named CS-5 and CS-6.

S2: Synthesis of sample for comparison

Pure copper for thermogravimetric analysis was synthesized as follows: 0.50 g $\text{CuSO}_4 \cdot 5\text{H}_2\text{O}$ was firstly dissolved in 100 mL H_2O , and then enough amount of $\text{N}_2\text{H}_4 \cdot \text{H}_2\text{O}$ was added into it under the protection of Ar gas. The as-prepared sediment was quickly collected and washed by centrifugation for several times, and then was dried in the vacuum oven for further use.

Glucose on copper foil after hydrothermal carbonization for Raman spectra was synthesized as follows: 1.0 g $\text{C}_6\text{H}_{12}\text{O}_6$ was firstly dissolved in 40 mL H_2O , and then together with a bare copper foil (1 cm * 2 cm), it was transferred into a 50 mL Teflon-lined stainless-steel autoclave and heated in oven at 200 °C for 24 hours. After hydrothermal process, the copper foil was collected and washed several times with deionized water, and then dried under vacuum at 65 °C for further characterization.

S3: Materials Characterization

Scanning electron microscopy (SEM) images and elemental analysis were recorded on field emission scanning electron microscopy (FEI Nova Nano SEM 450). Transmission electron microscopy (FEI Tecnai G2 F30) was used to characterize the high-resolution TEM (HRTEM) images. Atomic Force Microscope (AFM) images were recorded on NanoScope (R) III instrument operated in a tapping mode, and the sample was firstly dispersed in ethanol and then dropped on the fresh mica, and finally dried under vacuum at 65 °C. The X-ray diffraction (XRD, Rigaku D/Max 2500) with Cu-K α radiation was used for measurement of the crystallographic structure of as-prepared products. Thermogravimetric analysis (TGA) of samples was conducted on a TA Instruments Q600 with a heating rate of 10 °C min⁻¹ under air atmosphere, and the sample mass was about 10mg. Elemental analysis (EA) of samples was conducted on an elemental vario MAX cube (Elementar, GmbH), and the sample mass was about 200 mg, using aspartic acid as standard sample. X-ray photoelectron spectroscopy (XPS, PHI-1800) was introduced to characterize the change of surface elemental content in products by argon ion etching different time for 0, 10, 30, 50, 70 seconds. Raman spectra were recorded on Horiva (LabRam HR-800) spectrometer, the range of wave number was from 500 to 2500. High performance liquid chromatography (HPLC) was introduced to analysis the molecules in water solution after hydrothermal reaction. The solution was purified several times by centrifugation at 8000 rpm for 5 min, and without further dilute, 10 μ L sample was injected directly to analysis. As for analysis of furfural and hydroxymethylfurfural, LC-20AD (Shimadzu) with Ultimate Plus-C18 (4.6 * 150 mm, 3.5 μ m) was used, and the mobile phase was CH₃OH/H₂O (10/90 in volume) with a speed of 1.0 mL/min, and an ultraviolet detector (254 nm) was used for detection. As for analysis of glucose, maltose, fructose, and sucrose, Agilent 1260 with Ultimate XB-NH₂ (4.6 * 250 mm, 5 μ m) was used, and the mobile phase was CH₃CN/H₂O (70/30 in volume) with a speed of 1.0 mL/min, and a differential refractive index detector was used for detection.

S4: Structure of copper and composition of nanosheets

In order to investigate the structure of copper in the product, and considering carbon can be fully burned under air at the temperature of 500 °C, SEM was introduced to characterize the morphology of Product-2 both before and after thermal treatment for 2 h (Fig. S5). The results show that both the product and *in-situ* formed copper exhibit two-dimensional structure. For the experiment without adding CuSO₄·5H₂O, no carbon sheets but only bulk carbon or carbon micro-spheres is found (Fig. S6), indicating the *in-situ* formed copper with two-dimensional structure serves an important role.

To prove the nanosheets are composited mainly by carbon, typical EDS elemental mapping images are obtained in Fig. S7. Except for element of silicon and gold (originated from sample loading of silicon substrate and sample

coating of sputter gold), only carbon could be obviously found, indicating the successful preparation of two-dimensional carbon nanosheets. Similarly, carbon nanosheets with multilayered structure are also successfully prepared under temperature of 150, 200 and 250 °C (Fig. S8), which exhibit uniform size and distribution with no obvious impurities.

S5: Universal property and comparison with others' work

What's more, biomass of *Pachira aquatica* Aubl petioles (leaf stalks) and bamboo leaves are also taken as carbon precursor for hydrothermal experiments under 300 °C. Digital images of as-prepared product are shown in Fig. S10 (a-d), and similar to the results of experiments using *Pachira aquatica* Aubl leaves as carbon precursor, by characterizations of XRD (Fig. S10e), SEM (Fig. S11, S12 (a-d)), and Raman (Fig. S12e), it also indicates the successful preparation of two dimensional *in-situ* copper and multilayered graphitic carbon nanosheets.

In order to furtherly investigate what kind of small molecules may exist during the hydrothermal process, HPLC is introduced to analysis the water solution after hydrothermal reaction. As shown in Fig. S14, furfural, hydroxymethylfurfural, and glucose could be detected in the solution under hydrothermal temperature of 150 °C, and two small molecules of furfural and hydroxymethylfurfural could also be detected in the solution under hydrothermal temperature of 200 °C. These results show that biomass was hydrolyzed into small molecules during the hydrothermal process. The reason of no detection of some other small molecules under higher temperature is cause by furtherly carbonization after hydrolysis. In order to directly prove copper can be used for catalytic graphitization, glucose solution with one bare copper foil was put together for hydrothermal carbonization under 200 °C. As seen in Fig. S15, glucose was successfully carbonized, as well as graphitized.

Based on the above results, the synthesis mechanism could be summarized as follows: firstly, hydrolysis takes place and biomass polymers, such as cellulose and hemicellulose, disintegrate into their monomeric chains,¹ thus producing molecules² like furfural, hydroxymethylfurfural, glucose, maltose, fructose, and sucrose (Fig. S13), and as well as some acids³. Furtherly, with these molecules serving as reducing and capping agent, copper with two-dimensional structure is *in-situ* formed. After that, with copper as substrate, dehydration of carbohydrate to furfural or hydroxymethylfurfural, polymerization towards polyfurans and carbonization via further intermolecular dehydration take place.^{1,4,5} Finally, with the aids of copper as catalyst, aromatization takes place directly or via the way of (hydroxymethyl)furfural,^{5,6} thus forming the graphitic carbon.

Considering that all hexose sugars, including diverse biomass (glucose, xylose, maltose, sucrose, amylopectin, starch), no matter what their complexity, degrade into (hydroxymethyl)furfural, which finally condenses into carbon-like materials under hydrothermal conditions above 180 °C⁴, and the fact copper is one of the most used catalyst for

graphitization, this method could be universal for preparing carbon nanosheets using other biomass or saccharides.

Finally, comparison of various graphitic carbon prepared at relatively low temperature with others' work was also listed in Table S3, and it showed that this one-pot hydrothermal carbonization method for preparing graphitic carbon exhibited much lower temperature, as well as good advantages of facile process and environmentally friendly.

Table S1. Carbon content of as-prepared products determined by TGA and EA.

| Sample | TGA (wt %) | EA (wt %) |
|-----------|------------|-----------|
| Product-1 | 0.45 | 0.41 |
| Product-2 | 1.61 | 1.58 |
| Product-3 | 1.99 | 1.92 |
| Product-4 | 3.08 | 3.04 |

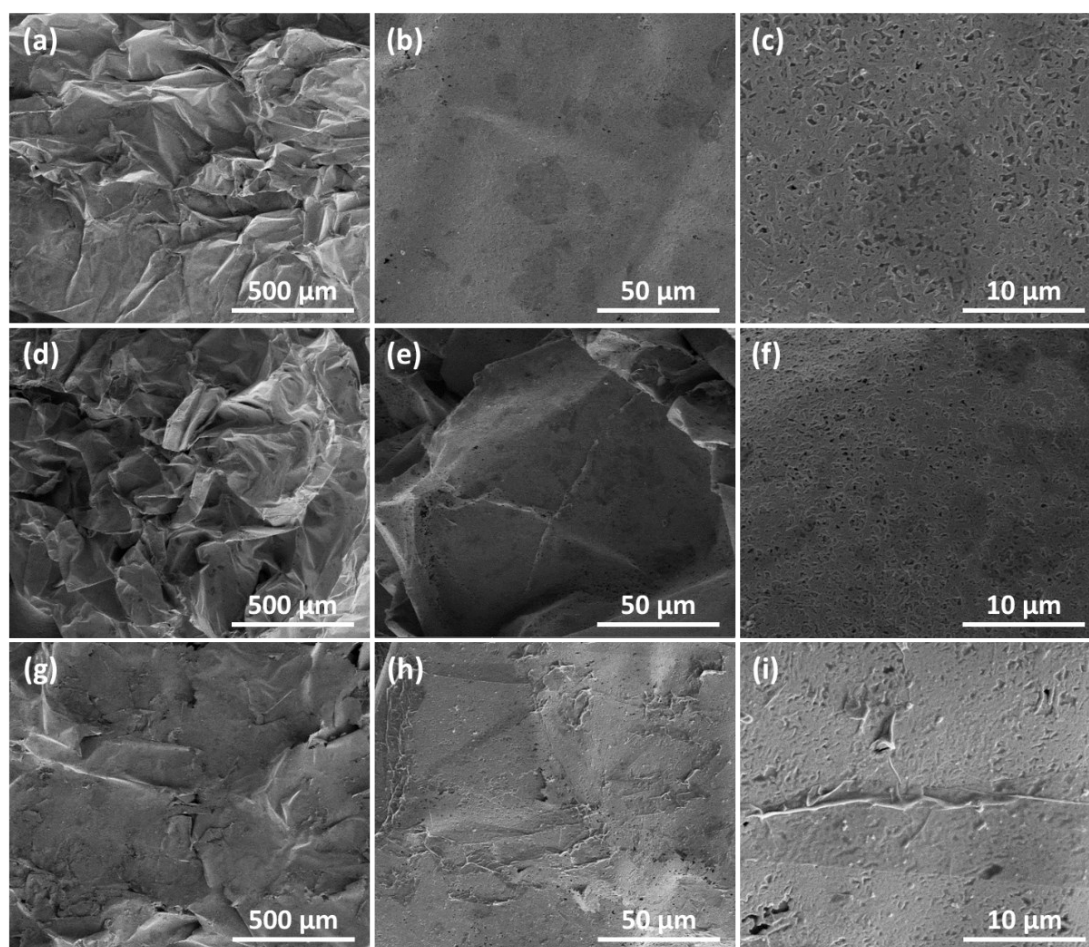


Figure S1. SEM images with different magnification of as-prepared product under different temperatures: (a-c) 150 °C, (d-f) 200 °C, (g-i) 250 °C.

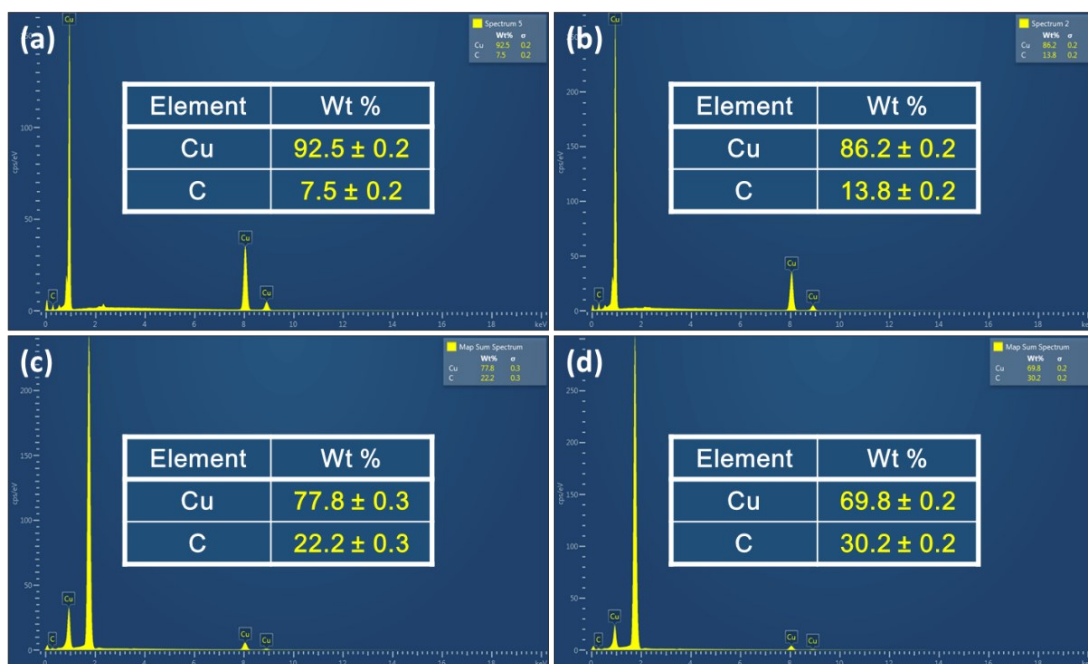


Figure S2. SEM-EDS analysis of as-prepared product under different temperature: (a) 150 °C, (b) 200 °C, (c) 250 °C, (d) 300 °C.

Table S2. Compositions of as-prepared products determined by SEM-EDS analysis.

| Sample | C Content (wt %) | Cu Content (wt %) | Weight ratio of C/Cu |
|-----------|------------------|-------------------|----------------------|
| Product-1 | 7.5 | 92.5 | 0.08 |
| Product-2 | 13.8 | 86.2 | 0.16 |
| Product-3 | 22.2 | 77.8 | 0.29 |
| Product-4 | 30.2 | 69.8 | 0.43 |

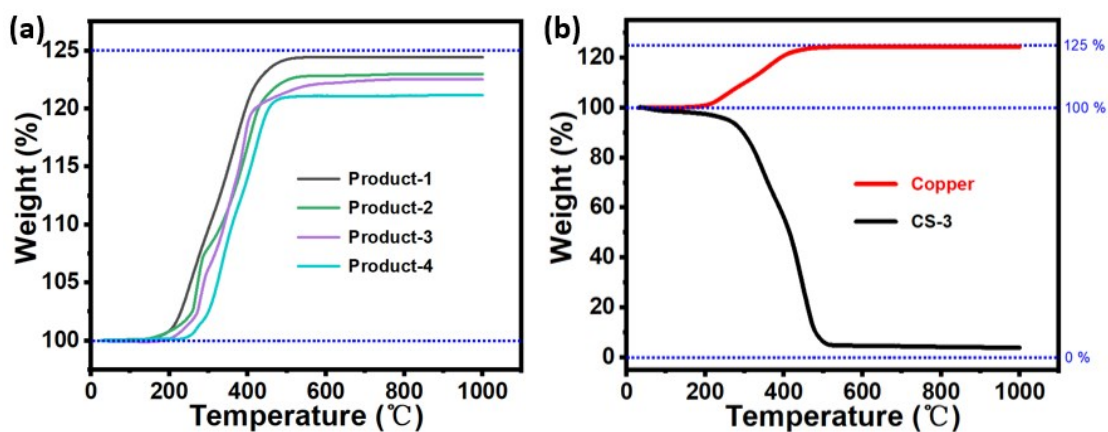


Figure S3. TGA analysis of (a) different as-prepared product and (b) samples of copper and CS-3.

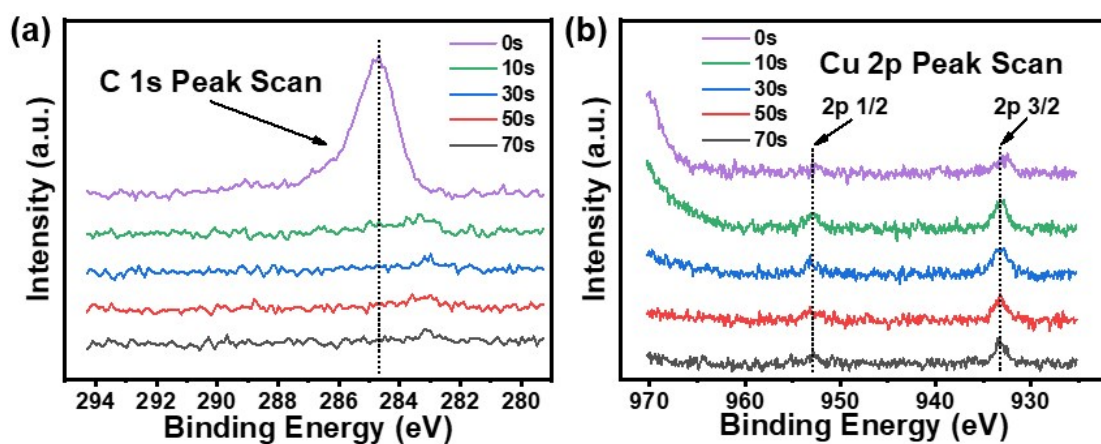


Figure S4. XPS peak scan of (a) C 1s and (b) Cu 2p of Product-3 at different etching time.

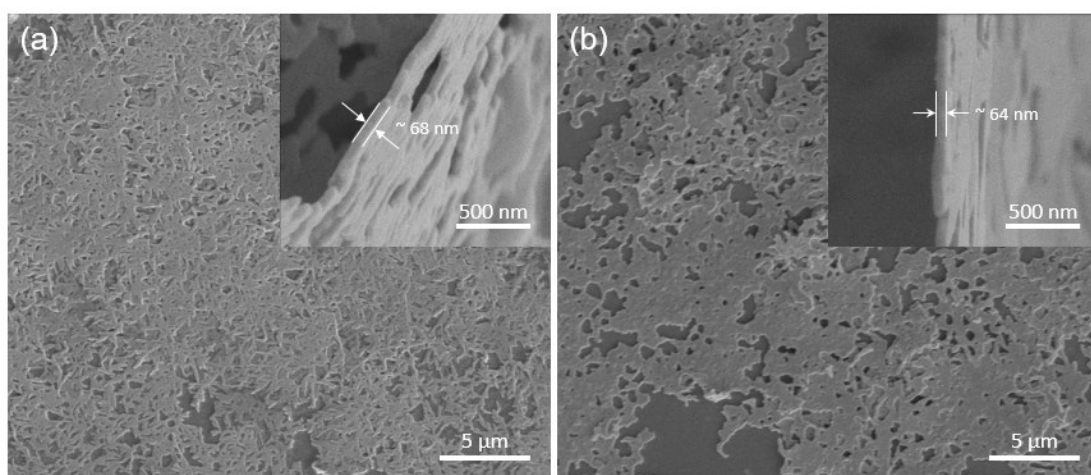


Figure S5. SEM images of Product-2 (a) before and (b) after thermal treatment at 500 °C for 2 hours.

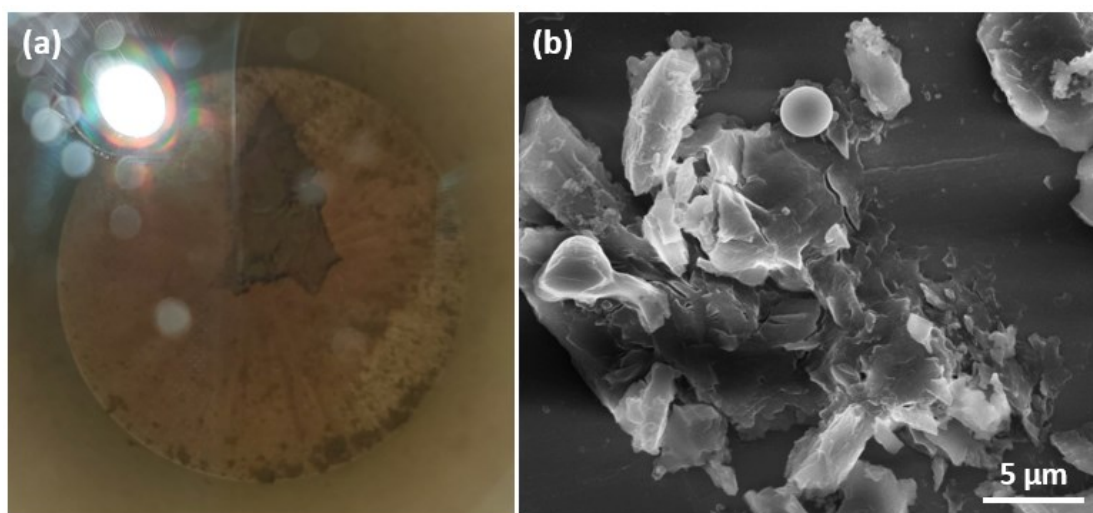


Figure S6. (a) Digital and (b) SEM images of as-prepared product by experiment without $\text{CuSO}_4 \cdot 5\text{H}_2\text{O}$.

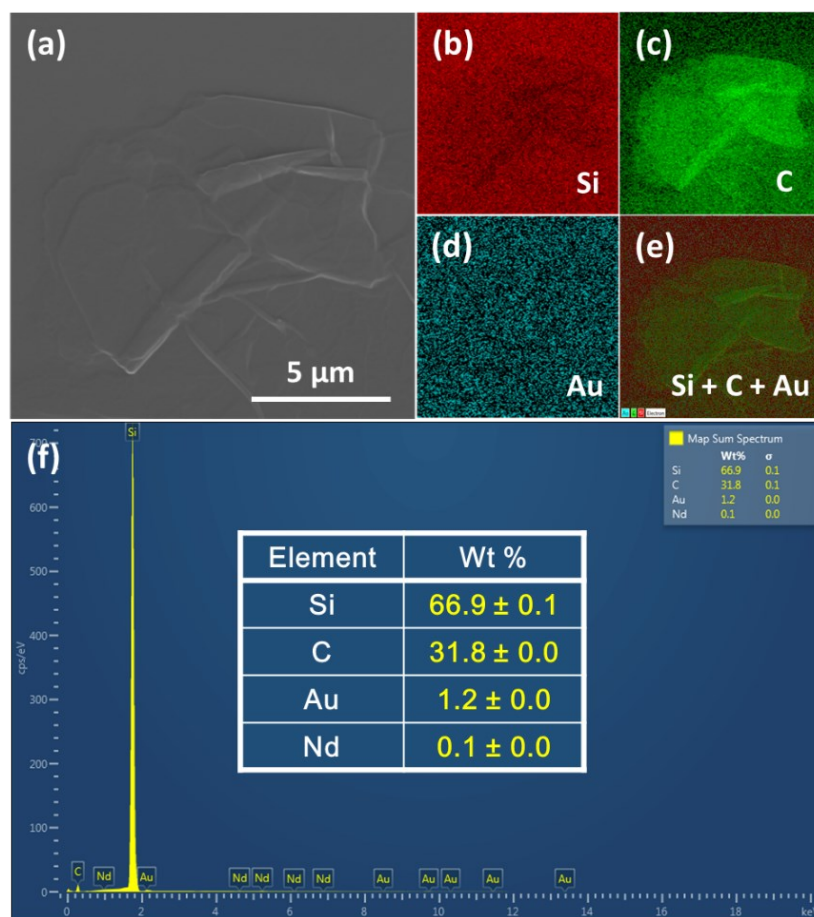


Figure S7. (a) SEM image, (b-e) EDS elemental mapping images and corresponding (f) EDS elemental analysis of as-prepared carbon sheets under the temperature of 300 °C.

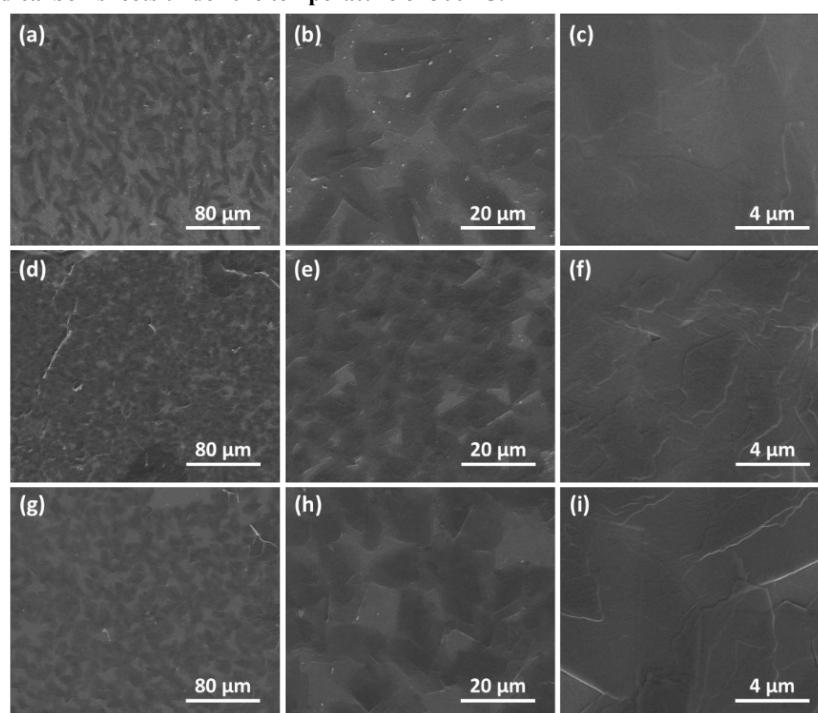


Figure S8. SEM images with different magnification of as-prepared carbon sheets under different temperatures: (a-c) 150 °C, (d-f) 200 °C, (g-i) 250 °C.

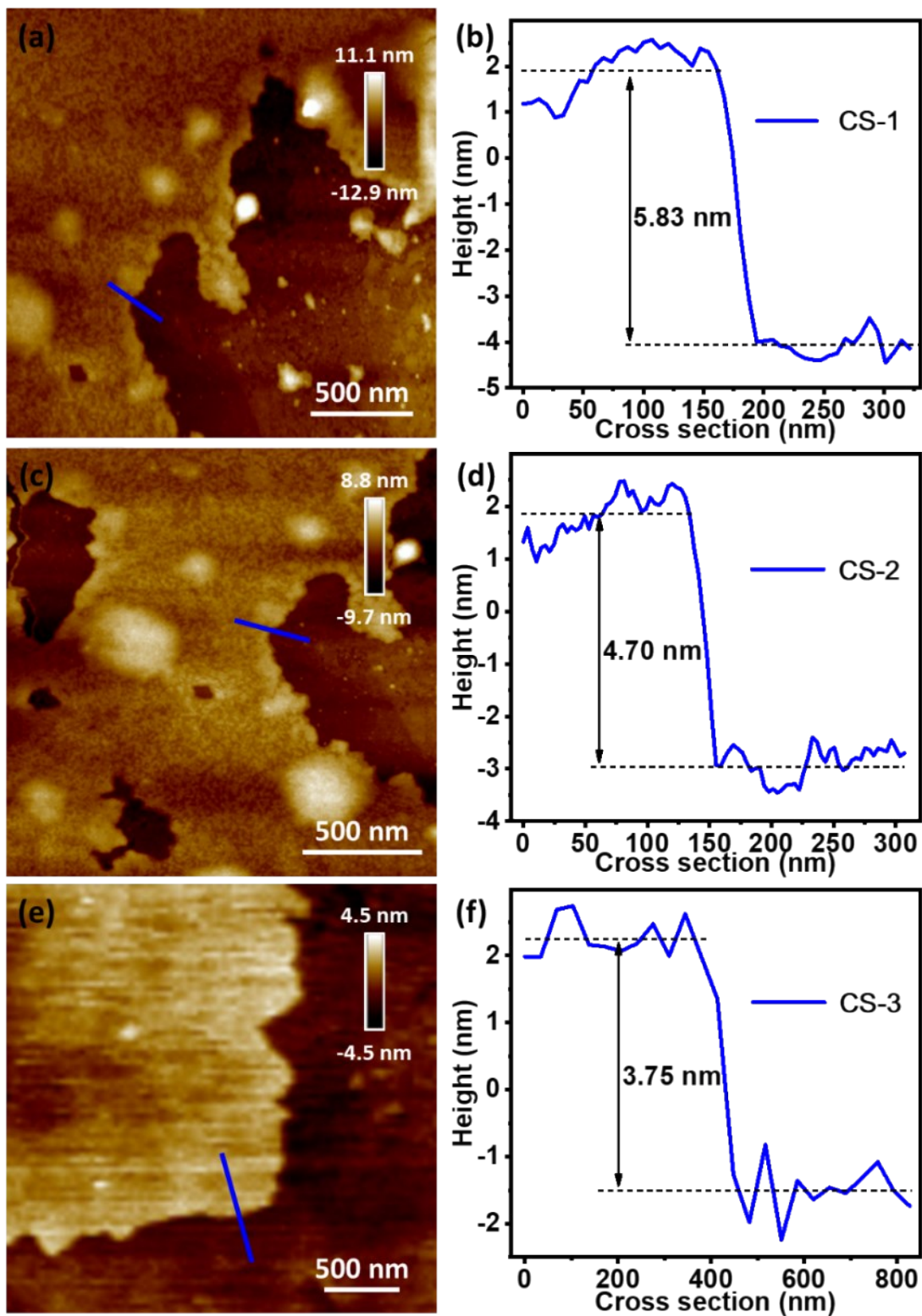


Figure S9. Typical AFM height images and corresponding height profile analysis of carbon sheets prepared under different temperatures: (a, b) 150 °C, (c, d) 200 °C, (e, f) 250 °C.

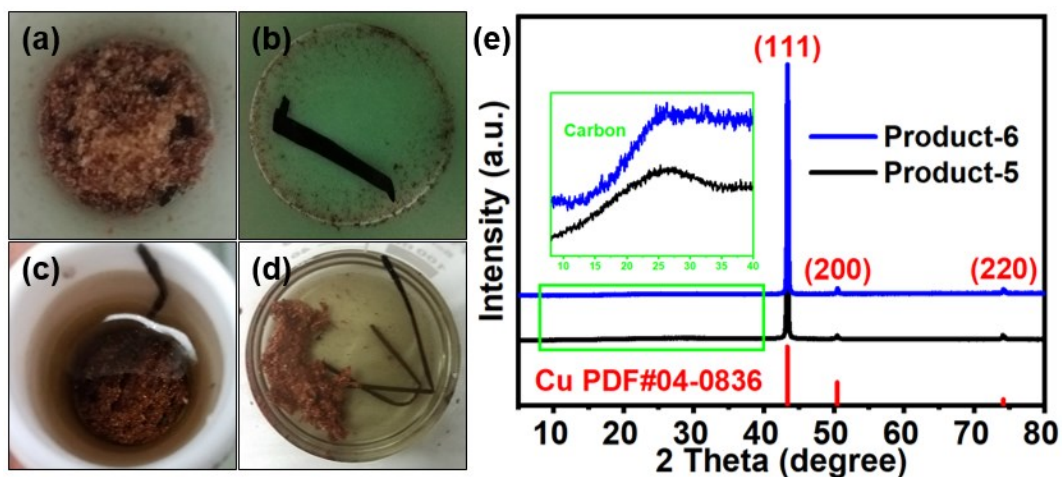


Figure S10. Digital images of as-prepared product by (a, b) bamboo leaves and (c, d) *Pachira aquatica* Aubl petioles. (e) XRD analysis of corresponding as-prepared product.

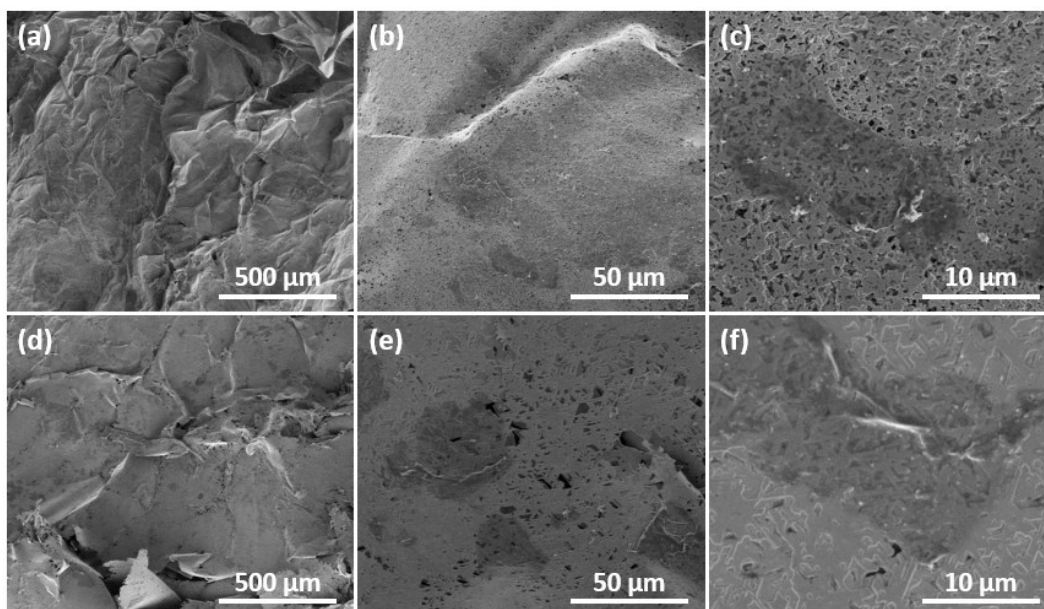


Figure S11. SEM images of as-prepared product by (a-c) bamboo leaves and (d-f) *Pachira aquatica* Aubl petioles.

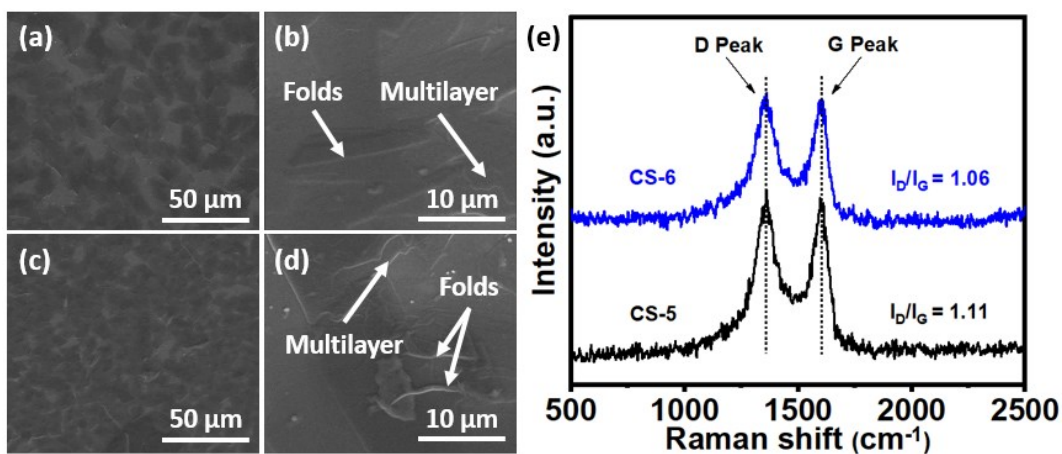


Figure S12. SEM images of obtained carbon sheets with carbon precursor of (a, b) bamboo leaves and (c, d) *Pachira aquatica* Aubl petioles. (e) Raman spectra of corresponding carbon sheets.

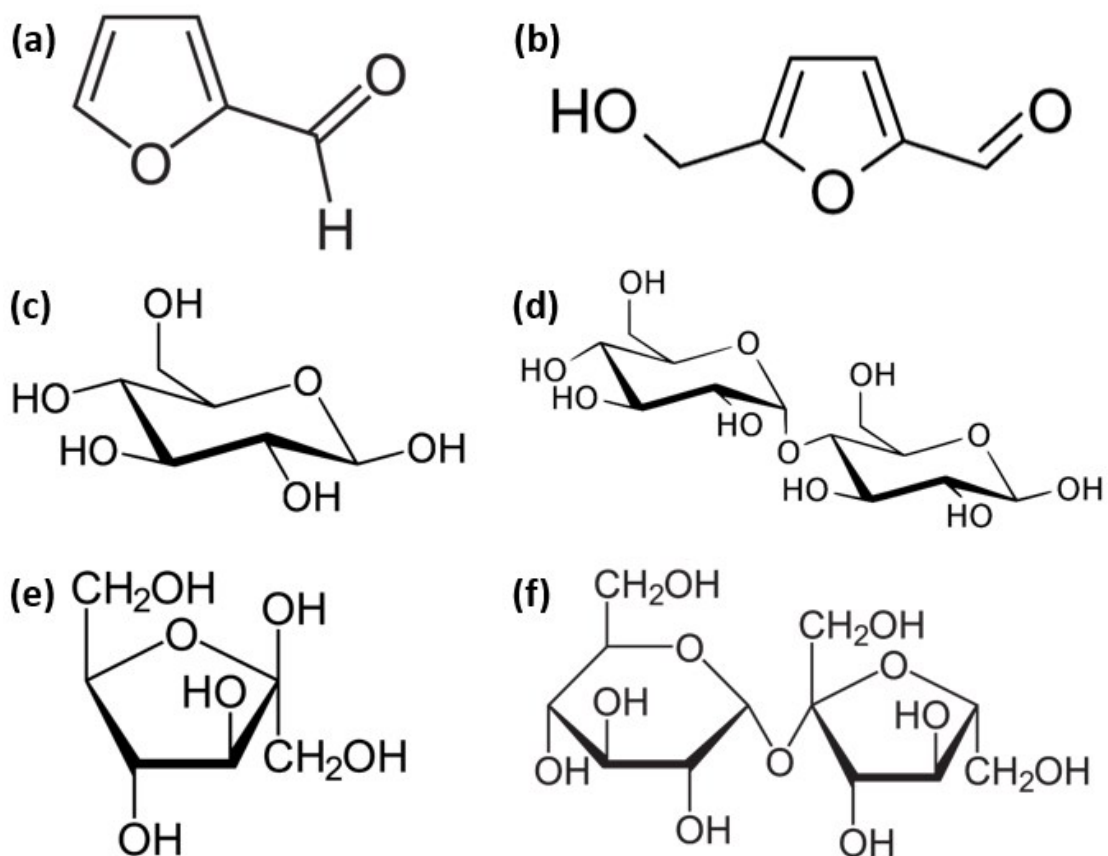


Figure S13. Chemical structure of different molecules: (a) Furfural, (b) Hydroxymethylfurfural, (c) Glucose, (d) Maltose, (e) Fructose, and (f) Sucrose.

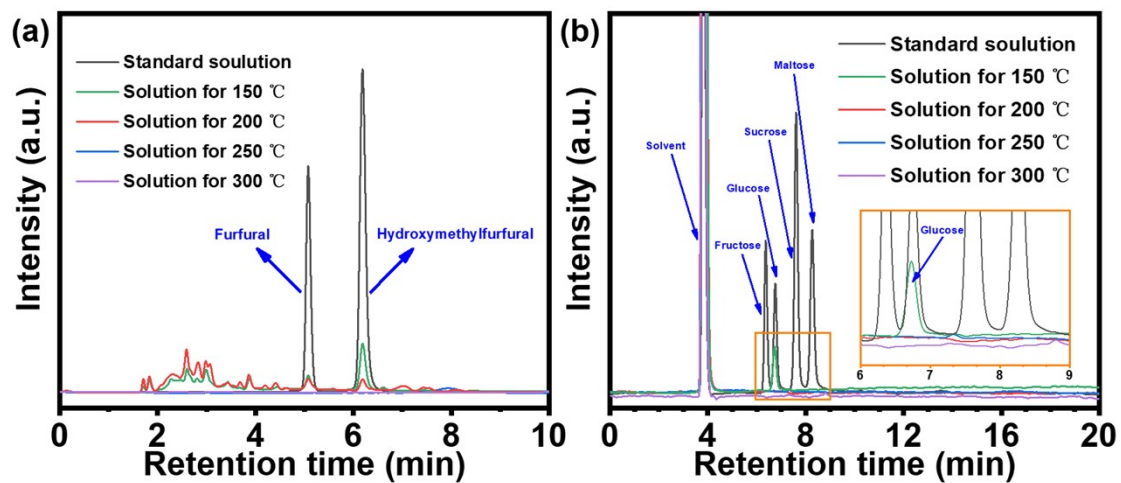


Figure S14. HPLC analysis of water solutions after hydrothermal carbonization at different temperatures.

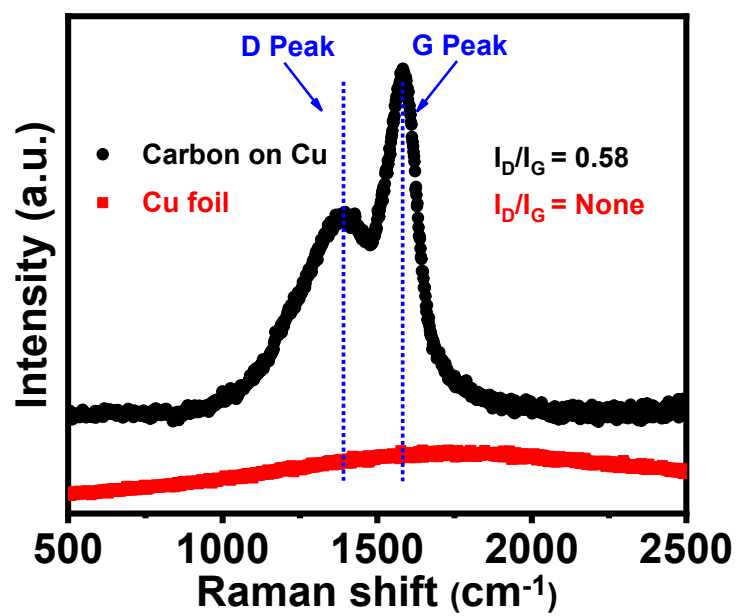


Figure S15. Raman spectra of bare copper foil and glucose on copper foil after hydrothermal carbonization at temperature of 200 °C.

Table S3. Comparison of various graphitic carbon prepared at relatively low temperature with others' work.

| Method | Conditions | Precursor | Reagent | Product | Refer. |
|----------------------------|---------------|--|---|-------------------------|--------------|
| Hydrothermal carbonization | 200-300 °C | leaf/petiole | <i>in-situ</i> formed Cu | graphitic nanosheets | This work |
| Pyrolysis | 600-900 °C | C ₂ H ₅ OH | <i>in-situ</i> formed Fe | graphitic nanocages | 7 |
| Hydrothermal and pyrolysis | ~200 & 900 °C | glucose/sucrose/starch | Ni(NO ₃) ₂ | graphitic nanocoils | 8 |
| Hydrothermal and pyrolysis | ~200 & 900 °C | sucrose | SiO ₂ , Fe(NO ₃) ₃ | graphitic carbon | 9 |
| Carbonization | 800-1200 °C | carbon nitride polymer(SBA-15) | CCl ₄ , C ₂ H ₄ (NH ₂) ₂ | graphitic carbon | 10 |
| Hydrothermal process | 800 °C | amorphous carbon | golden capsules | carbon nanotubes | 11 |
| Ion exchange and pyrolysis | 850 °C | carboxyl-containing polymer | Co(NO ₃) ₂ | graphitic carbon | 12 |
| CVD | 300-1000 °C | C ₆ H ₆ /PS/PMMA | H ₂ , Cu foil | graphene | 13 |
| CVD | 400-600 °C | PS | H ₂ /Ar, Cu/Ni foil | graphene | 14 |
| CVD | 800-1000 °C | PMMA/fluorene/sucrose | H ₂ /Ar, Cu/Ni foil | graphene | 15 |
| LPCVD | 600 °C | C ₆ H ₆ | H ₂ , Cu foil | graphene | 16 |
| LPCVD | 450-600 °C | C ₂ H ₂ | Au-Ni film | graphene | 17 |
| MPCVD | 450-750 °C | CH ₄ | H ₂ , Ni foil | graphene | 18 |
| PECVD | 400-600 °C | CH ₄ /C ₂ H ₄ | H ₂ , Si/SiO ₂ | graphene | 19 |
| PECVD | 650 °C | C ₂ H ₂ | H ₂ /Ar, Cu/Si/SiO ₂ | graphene | 20 |
| SWP-CVD | 300-400 °C | CH ₄ | H ₂ /Ar, Cu/Al foil | graphene | 21 |
| SWP-CVD | 450 °C | C ₂ H ₂ | H ₂ /Ar, Cu foil | graphene | 22 |

References

1. K. Tekin, S. Karagöz and S. Bektaş, *Renewable and sustainable Energy reviews*, 2014, **40**, 673-687.
2. M. Nagamori and T. Funazukuri, *Journal of Chemical Technology & Biotechnology: International Research in Process, Environmental & Clean Technology*, 2004, **79**, 229-233.
3. M. Möller, P. Nilges, F. Harnisch and U. Schröder, *ChemSusChem*, 2011, **4**, 566-579.
4. M.-M. Titirici and M. Antonietti, *Chemical Society Reviews*, 2010, **39**, 103-116.
5. A. Funke and F. Ziegler, *Biofuels, Bioproducts and Biorefining*, 2010, **4**, 160-177.
6. M.-M. Titirici, R. J. White, C. Falco and M. Sevilla, *Energy & Environmental Science*, 2012, **5**, 6796-6822.
7. J. N. Wang, L. Zhang, J. J. Niu, F. Yu, Z. M. Sheng, Y. Z. Zhao, H. Chang and C. Pak, *Chemistry of materials*, 2007, **19**, 453-459.
8. M. Sevilla and A. B. Fuertes, *Materials Chemistry and Physics*, 2009, **113**, 208-214.
9. J. B. Joo, Y. J. Kim, W. Kim, P. Kim and J. Yi, *Catalysis Communications*, 2008, **10**, 267-271.
10. K. K. Datta, V. V. Balasubramanian, K. Ariga, T. Mori and A. Vinu, *Chemistry—A European Journal*, 2011, **17**, 3390-3397.
11. J. M. Calderon Moreno and M. Yoshimura, *Journal of the American Chemical Society*, 2001, **123**, 741-742.
12. A.-H. Lu, W.-C. Li, E.-L. Salabas, B. Spliethoff and F. Schüth, *Chemistry of materials*, 2006, **18**, 2086-2094.
13. Z. Li, P. Wu, C. Wang, X. Fan, W. Zhang, X. Zhai, C. Zeng, Z. Li, J. Yang and J. Hou, *ACS nano*, 2011, **5**, 3385-3390.
14. M. Zhu, Z. Du, Z. Yin, W. Zhou, Z. Liu, S. H. Tsang and E. H. T. Teo, *ACS applied materials & interfaces*, 2016, **8**, 502-510.
15. Z. Sun, Z. Yan, J. Yao, E. Beitler, Y. Zhu and J. M. Tour, *Nature*, 2010, **468**, 549.
16. B. Zhang, W. H. Lee, R. Piner, I. Kholmanov, Y. Wu, H. Li, H. Ji and R. S. Ruoff, *ACS nano*, 2012, **6**, 2471-2476.
17. R. S. Weatherup, B. C. Bayer, R. Blume, C. Ducati, C. Baehz, R. Schlogl and S. Hofmann, *Nano letters*, 2011, **11**, 4154-4160.
18. Y. Kim, W. Song, S. Lee, C. Jeon, W. Jung, M. Kim and C.-Y. Park, *Applied physics letters*, 2011, **98**, 263106.
19. D. Wei, Y. Lu, C. Han, T. Niu, W. Chen and A. T. S. Wee, *Angewandte Chemie International Edition*, 2013, **52**, 14121-14126.
20. I. Jeon, H. Yang, S.-H. Lee, J. Heo, D. H. Seo, J. Shin, U.-I. Chung, Z. G. Kim, H.-J. Chung and S. Seo, *Acs Nano*, 2011, **5**, 1915-1920.
21. J. Kim, M. Ishihara, Y. Koga, K. Tsugawa, M. Hasegawa and S. Iijima, *Applied physics letters*, 2011, **98**, 091502.
22. G. Kalita, M. E. Ayhan, S. Sharma, S. M. Shinde, D. Ghimire, K. Wakita, M. Umeno and M. Tanemura, *Corrosion science*, 2014, **78**, 183-187.